Hindawi
Journal of Nanomaterials
Volume 2018, Article ID 6131085, 12 pages
https://doi.org/10.1155/2018/6131085

Research Article

Stabilization of Electrospun PAN/Gelatin Nanofiber Mats for Carbonization

Lilia Sabantina,[1,2] Daria Wehlage,[1] Michaela Klöcker,[1] Al Mamun,[3] Timo Grothe,[1] Francisco José García-Mateos,[2] José Rodríguez-Mirasol,[2] Tomás Cordero,[2] Karin Finsterbusch,[3] and Andrea Ehrmann[1]

[1]*Bielefeld University of Applied Sciences, Faculty of Engineering and Mathematics, Bielefeld, Germany*
[2]*Universidad de Málaga, Andalucía Tech, Dpto. de Ingeniería Química, Málaga, Spain*
[3]*Niederrhein University of Applied Sciences, Mönchengladbach, Germany*

Correspondence should be addressed to Andrea Ehrmann; andrea.ehrmann@fh-bielefeld.de

Received 18 April 2018; Accepted 30 August 2018; Published 21 October 2018

Academic Editor: Sung Hoon Jeong

Due to their electrical and mechanical properties, carbon nanofibers are of large interest for diverse applications, from batteries to solar cells to filters. They can be produced by electrospinning polyacrylonitrile (PAN), stabilizing the gained nanofiber mats, and afterwards, carbonizing them in inert gas. The electrospun base material and the stabilization process are crucial for the results of the carbonization process, defining the whole fiber morphology. While blending PAN with gelatin to gain highly porous nanofibers has been reported a few times in the literature, no attempts have been made yet to stabilize and carbonize these fibers. This paper reports on the first tests of stabilizing PAN/gelatin nanofibers, depicting the impact of different stabilization temperatures and heating rates on the chemical properties as well as the morphologies of the resulting nanofiber mats. Similar to stabilization of pure PAN, a stabilization temperature of 280°C seems suitable, while the heating rate does not significantly influence the chemical properties. Compared to stabilization of pure PAN nanofiber mats, approximately doubled heating rates can be used for PAN/gelatin blends without creating undesired conglutinations, making this base material more suitable for industrial processes.

1. Introduction

Functional nanofibers are used in a broad variety of applications, from nanofibrous membranes for filters [1] to substrates in tissue engineering [2, 3] to electrocatalysis [4], capacitors [5], and other applications based on the conductivity of the nanofibers [6]. Especially for batteries and other energy applications, often carbon nanofibers are used [7–11].

Such carbon nanofibers are often prepared via the electrospinning route, followed by stabilization and afterwards carbonization. Both steps influence the morphologies, the mechanical and electrical properties of the final carbon nanofibers significantly. While carbon nanofibers can be produced from a broad variety of materials [12–14], one of the most common materials for this purpose is polyacrylonitrile (PAN). PAN changes fiber diameters and mat morphologies significantly for varying spinning and solution parameters [15, 16], while the fibers themselves keep their flat, even surfaces.

In most applications, however, it is advantageous to further increase the surface: volume ratio of the nanofibers. This can be done by blending PAN with other polymers or inorganic material, a method which may also alter other physical properties, such as the conductivity. Increased crystallinity and conductivity were found, e.g., when PAN/pitch nanofibers were carbonized [17]. Blending PAN with cellulose acetate resulted in increased adsorption properties of the carbonized nanofibers [18]. Combined with diverse water-soluble polymers, only gelatin showed a significant influence on the PAN fiber diameters [19]. PAN/gelatin blends have also shown to create highly porous fibers by electrospinning [20]. Nevertheless, to the best of our knowledge,

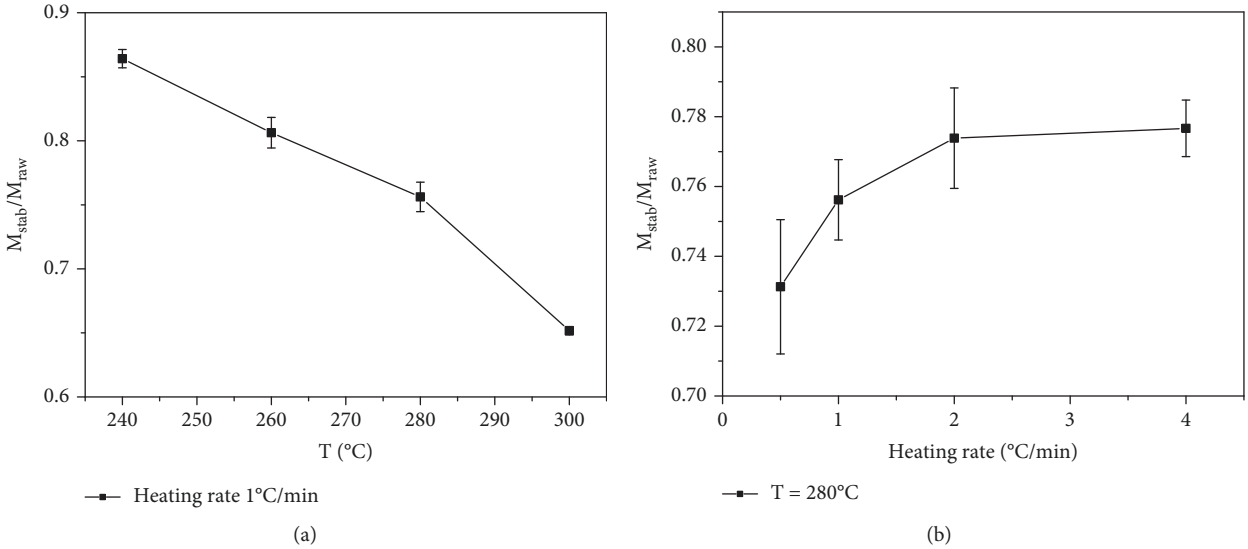

Figure 1: Normalized masses after stabilization at different temperatures (a) and using different heating rates (b).

no investigations on the stabilization of such electrospun PAN/gelatin nanofiber mats were performed yet.

In this paper, we report on the influence of the stabilization temperatures and heating rates on the chemical properties and morphologies of the resulting nanofiber mats.

2. Materials and Methods

Electrospinning was performed with a "Nanospider Lab" (Elmarco, Czech Republic), a needleless electrospinning machine based on the wire technology, using a polypropylene fiber mat as the substrate. The spinning parameters were high voltage 70 kV, nozzle diameter 1.5 mm, carriage speed 100 mm/s, ground-substrate distance 240 mm, electrode-substrate distance 50 mm, temperature in chamber 22°C, and relative humidity in chamber 33%.

The spinning solution contained 16% PAN in DMSO (min 99.9%, purchased from S3 Chemicals, Germany) and 9% gelatin (Abtei, Germany).

Samples of 50 mm × 50 mm of the electrospun nanofiber mats were stabilized in a muffle furnace B150 (Nabertherm), approaching stabilization temperatures between 240°C and 300°C at heating rates between 0.5°C/min and 4°C/min, and then 1 h of isothermal treatment at the final temperature. For each combination of heating rate and temperature, samples were stabilized with their borders fixed by placing a metal frame with sufficient weight on them as well as freely, without any fixation. Carbonization was performed in a furnace CTF 12/TZF 12 (Carbolite Gero Ltd., Hope, UK), approaching a temperature of 800°C with a heating rate of 10°C/min in a nitrogen flow of 150 mL/min (STP), followed by isothermal treatment for 1 h.

Masses of the samples were taken before and after stabilization using an analytical balance (VWR). Samples dimensions were analyzed by the program ImageJ 1.51j8.

For Fourier-transform infrared (FTIR) spectroscopy, an Excalibur 3100 (Varian, Inc.) was used. Color measurements were performed with a sph900 spectrometer (ColorLite). Scanning electron microscopy (SEM) images were taken by a Zeiss 1450VPSE with a resolution of 5 nm or a JSM-840 microscope, respectively, using a nominal magnification of 5000x. Optical images of the nanofiber mats were taken using a confocal laser scanning microscope (CLSM) VK-100 with a nominal magnification of 2000x.

3. Results and Discussion

Figure 1 depicts the relative mass changes for different stabilization temperatures (Figure 1(a)) and different heating rates (Figure 1(b)), respectively. The trend of smaller normalized masses, i.e., larger losses, for higher stabilization temperatures is clearly visible. Compared to a previous study on pure PAN nanofiber mats, the normalized masses here are generally smaller, and the mass loss is strongly increased for higher temperatures. This indicates clearly the influence of the gelatin in the fibers—since gelatin denaturalizes around 40–90°C, depending on the water content [21], and it can be expected to be released from the nanofibers as long as it is not completely embedded in the fiber.

Opposite to mass measurements on stabilized PAN nanofibers, showing an approximately constant value of ~85% of the original mass, here, a clear heating rate dependence is visible for the lower heating rates. This suggests that here the duration of the heating time plays an important role, i.e., the lower the heating rate, the higher the polymer decomposition obtained due to pyrolysis and recombination reactions.

Besides the masses, the areas of the stabilized samples in fixed and unfixed states were measured. The results are depicted in Figure 2, depending on the temperature (Figure 2(a)) and the heating rate (Figure 2(b)), respectively. The ratio of the areas of the unfixed and the fixed samples decreases with increasing temperature as well as with increasing heating rate, showing that high temperatures and large heating rates cause more stress in the unfixed samples and let them crumple stronger than under less extreme

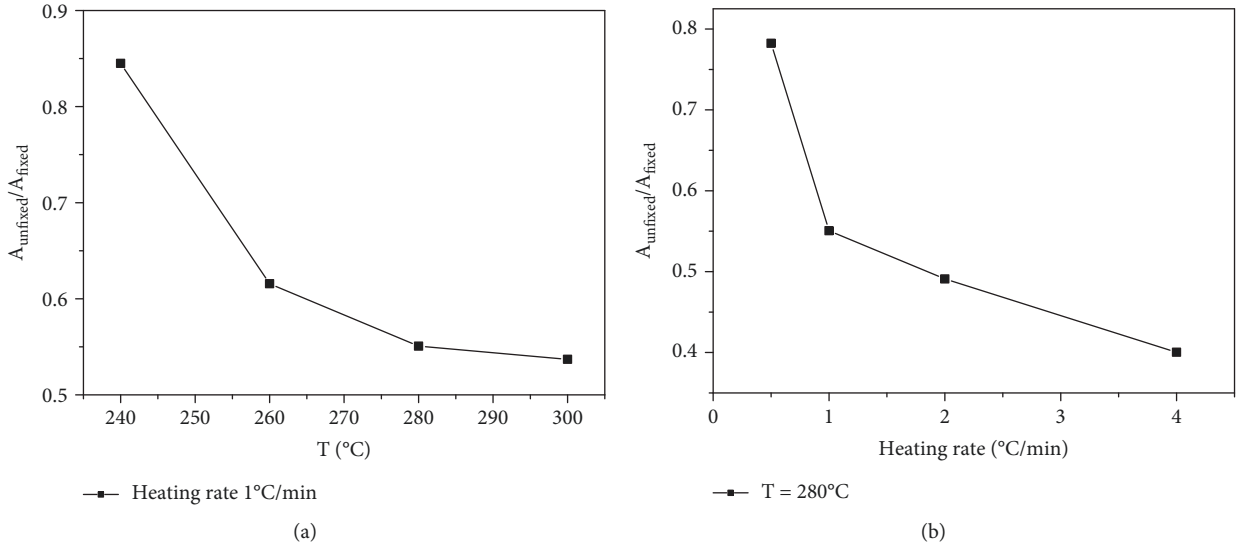

Figure 2: Normalized areas after stabilization at different temperatures (a) and using different heating rates (b).

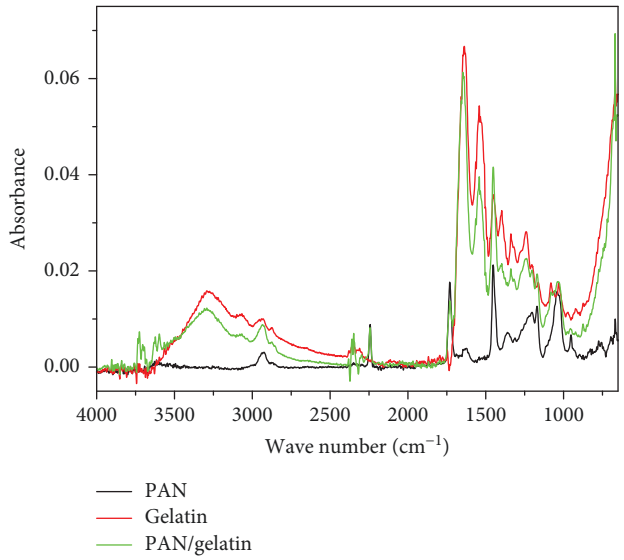

Figure 3: FTIR measurements on PAN, gelatin, and PAN/gelatin nanofiber mats.

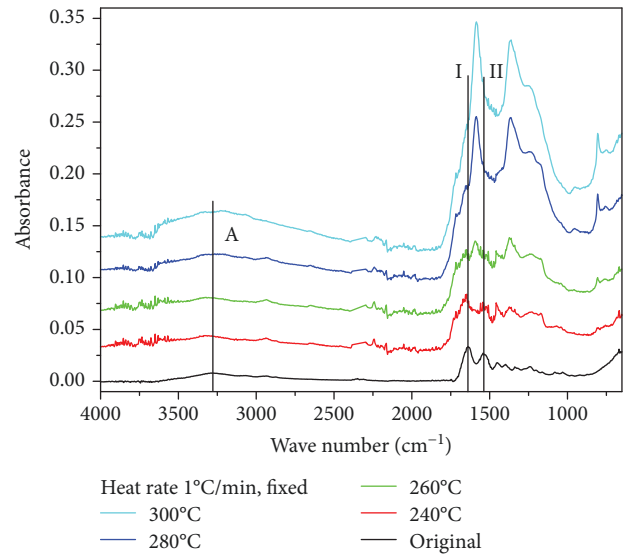

Figure 4: FTIR absorbance measurements on fixed samples, stabilized at different temperatures approached with 1°C/min. The lines are offset vertically for clarity.

conditions. This finding underlines the importance of fixing the samples during stabilization.

FTIR measurements were performed on the PAN/gelatin nanofiber mat before stabilization. Figure 3 shows the result together with pure PAN and pure gelatin nanofiber mats. Comparing the spectra shows that the PAN/gelatin line is composed of the typical PAN peaks in the range between 950 cm^{-1} and 1700 cm^{-1}, at 2240 cm^{-1} and 2938 cm^{-1} [22, 23] as well as gelatin peaks. The latter can be differentiated into the region around 2700–3600 cm^{-1} which is attributed to the amides A and B, the region around 900–1900 cm^{-1} showing the amides I, II, and III, and finally the region below 900 cm^{-1} depicting amide IV [24]. It should be mentioned that several peaks are hard to distinguish between pure PAN and pure gelatin. The most prominent peaks which are not existent in pure PAN are the peak around 3400 cm^{-1}, corresponding with amide A, and the peak near 700 cm^{-1}, corresponding to amide IV. In the original state after electrospinning, there are also clear differences between PAN and gelatin around 1640 cm^{-1} (amide I) and 1540 cm^{-1} (amide II); however, it is well known that in this region, significant changes will occur during the stabilization process, making these peaks possibly less suitable for the examination whether gelatin stays in the fabric during stabilization.

A comparison of the FTIR measurements on PAN/gelatin samples, heated at 1°C/min to different stabilization temperatures, is given in Figure 4. At first glance, the results look very similar to those gained by stabilizing pure PAN

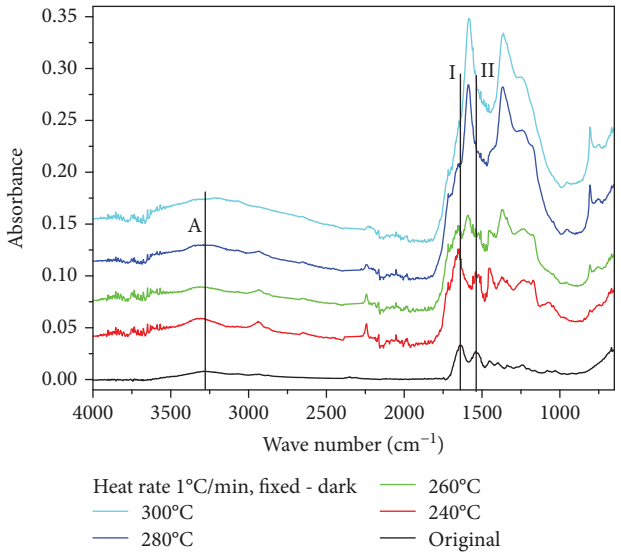

Figure 5: FTIR absorbance measurements on the dark areas on the back of fixed samples, stabilized at different temperatures approached with 1°C/min. The lines are offset vertically for clarity.

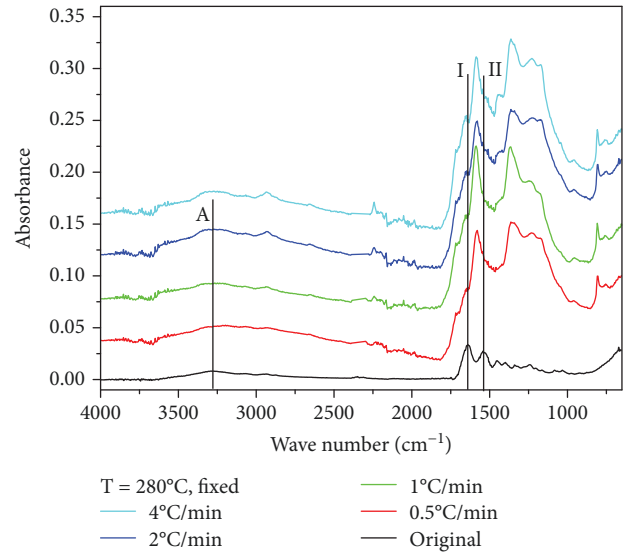

Figure 6: FTIR absorbance measurements on the dark areas on the back of fixed samples, stabilized at 280°C, approached with different heating rates. The lines are offset vertically for clarity.

nanofiber mats [23, 24]. Following the most prominent peaks of the original PAN/gelatin peaks shows that during stabilization (amides A, I, and II, as marked in Figure 4), there is no evidence for residual gelatin in the stabilized fiber mat. The same results are visible for the not fixed samples.

Optical examination of the samples after taking them out of the muffle oven revealed dark, nearly black areas on the back in the areas which had touched the underground during stabilization. Since the gelatin is no longer visible in the FTIR measurements taken on the upper surface of the samples, it can be assumed that gelatin—which decomposes above approx. 100°C but needs more than approx. 500°C for complete combustion—has precipitated here after melting. Figure 5 thus depicts FTIR scans of these dark areas.

While for a stabilization temperature of 240°C, the peaks for amides A and I are still clearly visible, they are superposed by the growing PAN stabilization peaks for higher temperatures. Thus, the FTIR results can in this case not clearly state which material causes the black areas on the back.

Figure 6 shows the heating rate dependence of PAN/gelatin nanofiber mats, stabilized at 280°C. While stabilizing pure PAN revealed significant differences in the FTIR measurements for different heating rates [25], here, all curves are very similar. A closer look, however, shows that for higher heating rates, the peaks for the amides A, I, and II stay visible, although strongly superposed by the large peaks of the stabilized PAN in these areas. This indicates that faster heating allows the gelatin to stay in the nanofiber mat to a certain amount. Similar results were found on the dark back of these samples (not shown here).

Optical investigations were performed, using a CLSM. Figure 7 depicts a comparison of an original PAN/gelatin nanofiber mat (Figure 7(a)) and a sample stabilized in fixed position at 280°C, approached at 1°C/min (Figure 7(b)).

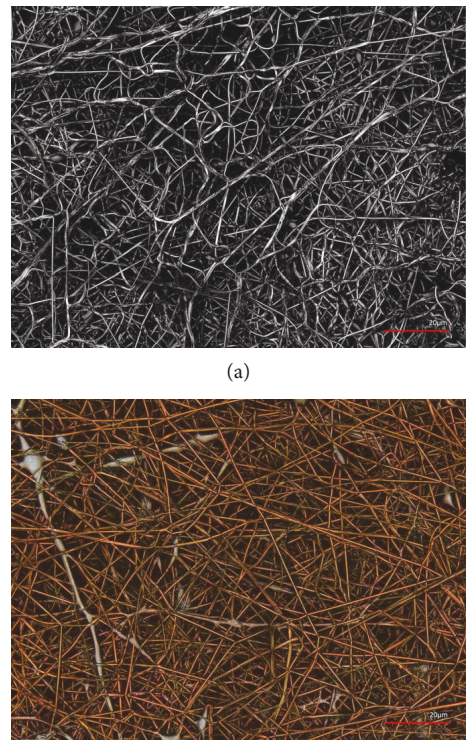

(a)

(b)

Figure 7: CLSM images of an untreated PAN/gelatin nanofiber mat (a) and a sample stabilized at 280°C, approached at 1°C/min (b). The scale bars indicate 20 μm.

Firstly, both images show the typical relatively thick and straight fibers which are typical for gelatin or PAN/gelatin [19]. After stabilization, the usual brown color of the stabilized PAN is visible. Here, however, some silvery fibers can be recognized, clearly indicating gelatin. It should be

Table 1: CLSM images of PAN/gelatin nanofiber mat, stabilized in fixed (left panels) and unfixed state (right panels) at different temperatures, approached with 1°C/min. For a better overview, the scale bars here indicate 50 μm.

	Fixed	Unfixed
240°C	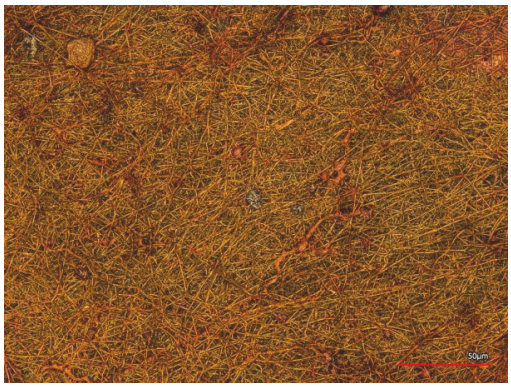	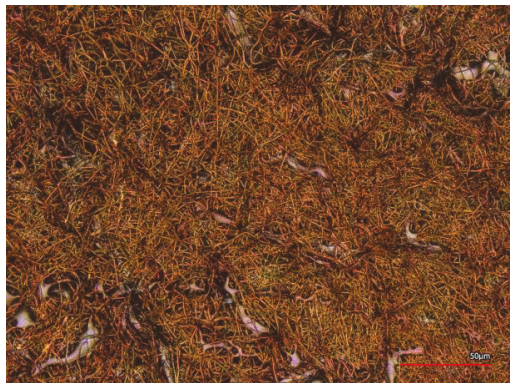
260°C		
280°C	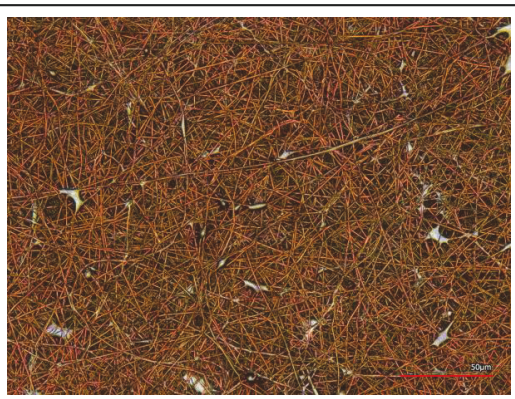	
300°C	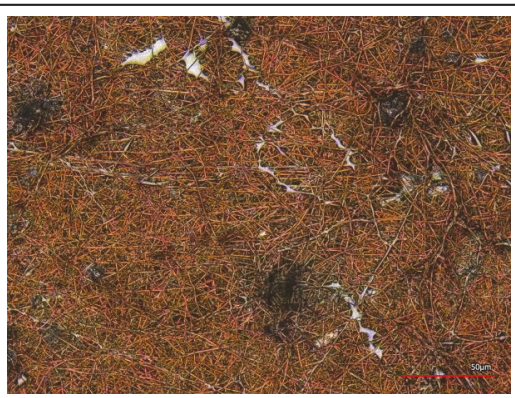	

Table 2: CLSM images of PAN/gelatin nanofiber mat, stabilized in fixed (left panels) and unfixed state (right panels) at 280°C, approached with different heating rates. The scale bars indicate 50 μm.

	Fixed	Unfixed
1°C/min	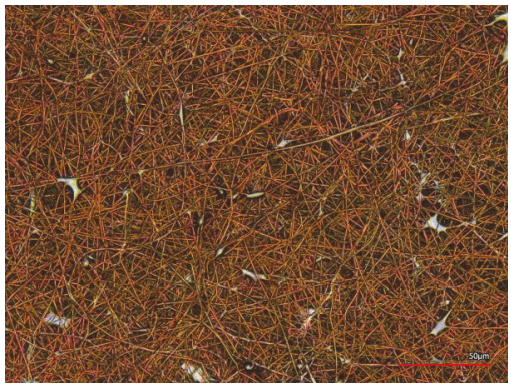	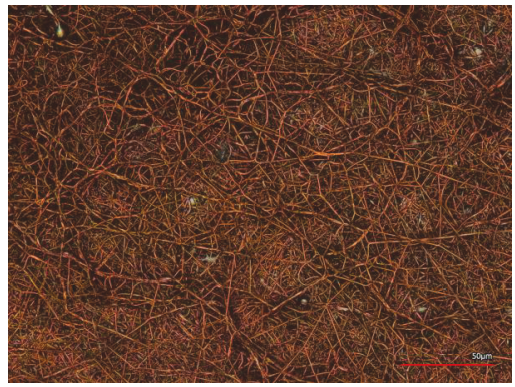
2°C/min	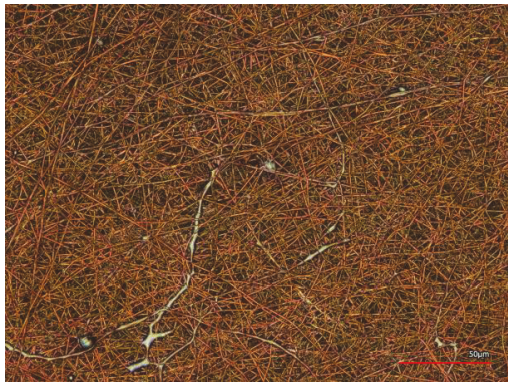	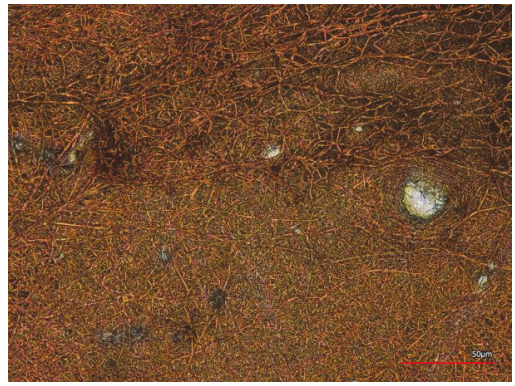
4°C/min	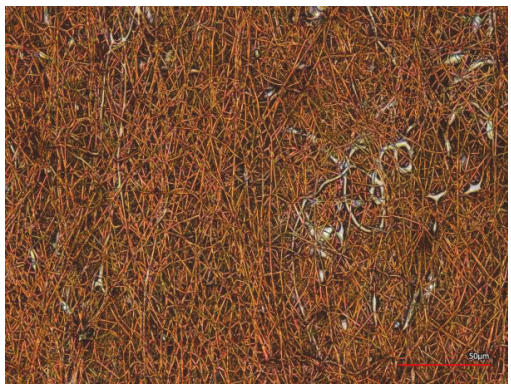	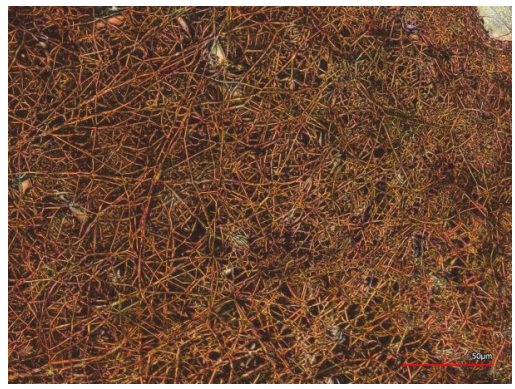

mentioned that—opposite to stabilization of pure PAN—the stabilization process here seems to straighten the fibers. Another important remark is that no undesired conglutinations are visible in the stabilized sample, as opposed to the stabilization process of pure PAN under identical conditions.

Table 1 compares the samples stabilized at different temperatures, approached with 1°C/min, in fixed and unfixed state. Firstly, most images show some areas in which silvery regions or fibers are visible which can clearly be attributed to gelatin since stabilized PAN shows a strong color change. Second, the typical crumpling of pure PAN fibers during stabilization is invisible for the fixed samples and severely reduced for the unfixed samples. This finding is independent from the stabilization temperature, thus possibly allowing using higher stabilization temperatures without a problematic influence on the nanofiber dimensions.

This observation shows clearly that blending PAN with gelatin can help to gain straight, long carbon nanofibers, as desired for most technical applications.

Table 2 depicts the dependence of the nanofiber mat morphology after stabilization at 280°C, approached with different heating rates. For the higher heating rates, the more chaotic fiber distribution for the unfixed samples is visible; however, still, no undesired conglutinations seem to appear. The assumption due to Figure 6 that faster heating leads to more remaining gelatin cannot be verified or falsified from these images, especially since gelatin inside

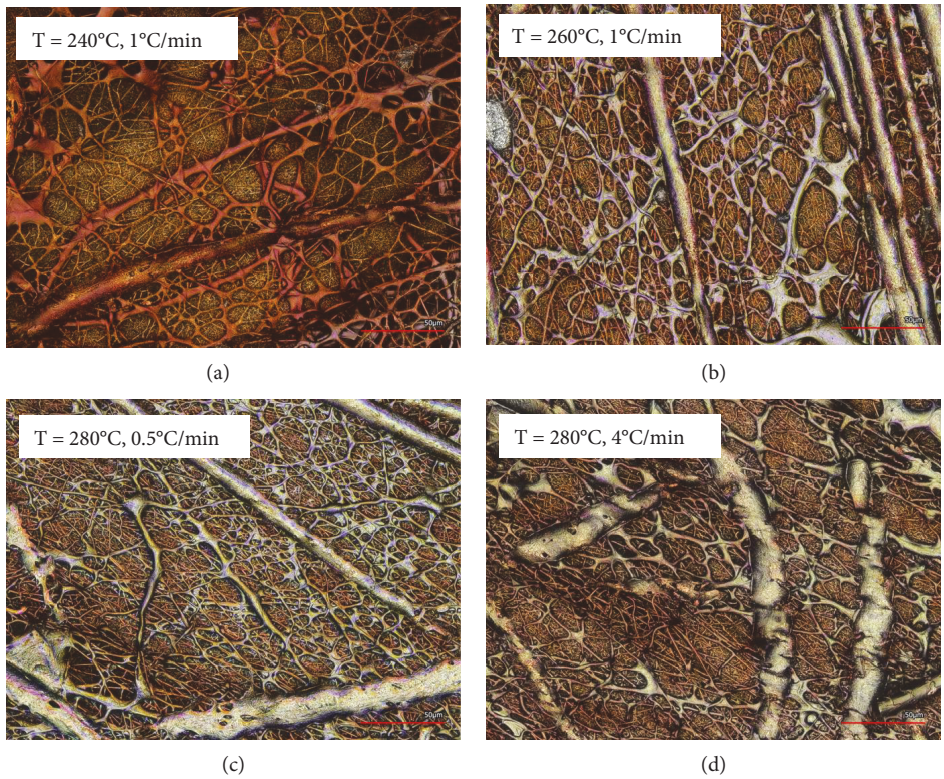

Figure 8: CLSM images of the back of different samples (see insets), stabilized under fixed conditions. The scale bars indicate 50 μm.

PAN fibers or blended fibers cannot be distinguished from pure PAN fibers.

All samples were also investigated from the back, where residual gelatin was expected due to the dark color and the slight differences in the FTIR spectra. Some results of fixed samples are depicted in Figure 8.

Firstly, a significant color change from 240°C to 260°C can be recognized. This fits well to the starting point of the main thermal degradation zone of gelatin reported in the literature [26, 27]. Thermal degradation between 250°C and 600°C includes breakage of protein chains and rupture of peptide bonds, involving the evolution of volatile compounds and formation of new C-C and C-N bonds in the solid matrix.

Independent from this finding, in all cases (including the images not shown here), a mixture of broad gelatin bands and fine gelatin membranes connecting PAN fibers can be identified. No clear influence of the heating rate or the temperature (as long as it is higher than 240°C) is visible.

These images show that a stabilization process using hanging samples, without contact to the underground, may be favorable to reduce these large gelatin agglomerations. On the other hand, it should be mentioned that the next step, carbonization of the samples, is usually performed at temperatures higher than 600°C so that gelatin will most probably completely be degraded after the carbonization process. Nevertheless, the influence of such gelatin agglomerations on the morphology of carbonized nanofiber mats should be investigated in the future.

Next, the morphology of the fibers themselves was investigated using SEM. The results for different temperatures are depicted in Table 3, while Table 4 shows the influence of different heating rates.

In all cases, the unfixed samples show stronger meandering of the fibers, an effect which is supported by high temperatures and high heating rates. Stabilization of fixed nanofiber mats results in most cases in straight, even fibers. Similar to the CLSM images, some gelatin fibers are still visible between the thinner PAN fibers. For the highest temperature and the highest heating rates, the fixed PAN fibers seem to be more irregular; thus, the SEM images suggest stabilization at 280°C (which is sufficient for stabilization, based on the FTIR results) and 1°C/min which is twice as high as the best stabilization temperature for pure PAN nanofiber mats of 0.5°C/min. It must be mentioned that the original aim of this study, creation and stabilization of PAN/gelatin nanofibers with porous surfaces, was not reached here, while the investigation gives a new approach to create smoother, more even fibers which can be stabilized with a higher heating rate than pure PAN nanofibers.

Finally, spectroscopic examinations of the stabilized nanofiber mats were performed. The color differences for the brighter front and the darker back compared to the original white nanofiber mat are depicted in Figure 9.

The difference between the dark and the "normal" areas is also visible in these measurements for all temperatures and heating rates. Interestingly, the maximum color difference is achieved at 280°C and decreases again at 300°C. This may be attributed to structural effects due to the degradation of gelatin. This explanation corresponds to the slightly increasing color differences with

Table 3: SEM images of PAN/gelatin nanofiber mat, stabilized in fixed (left panels) and unfixed state (right panels) at different temperatures, approached with 1°C/min. All images were taken using a nominal magnification of 5000x.

	Fixed	Unfixed
240°C	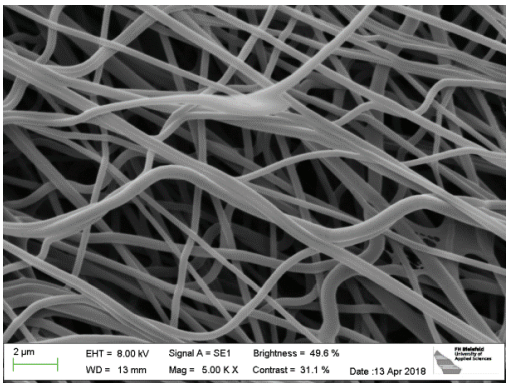	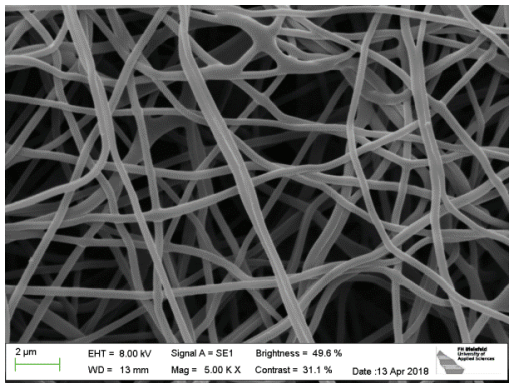
260°C	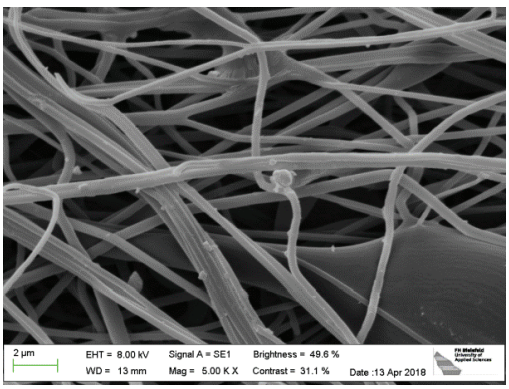	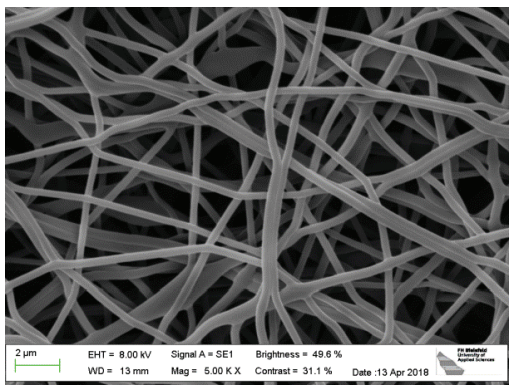
280°C	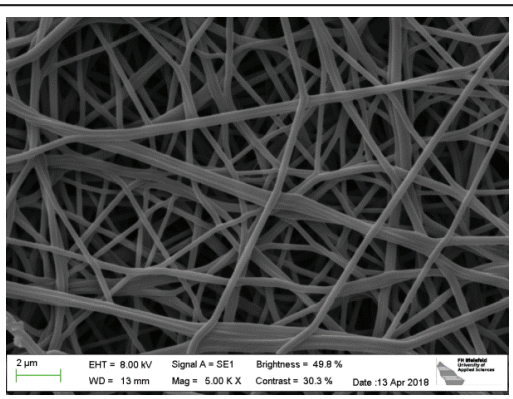	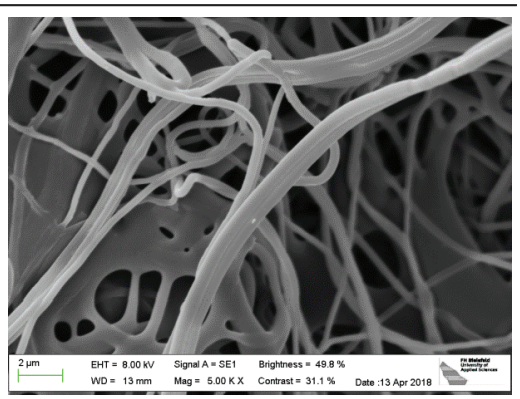
300°C	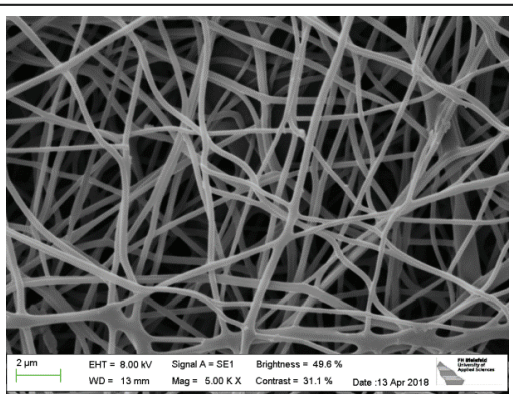	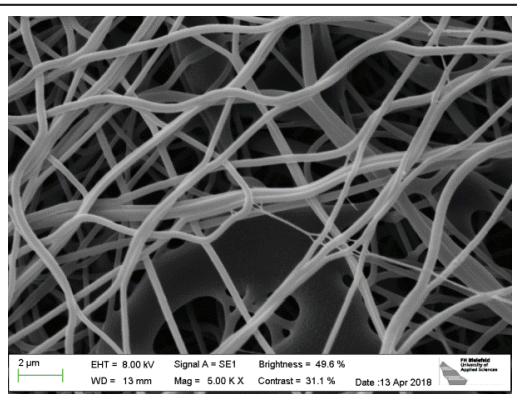

Table 4: SEM images of PAN/gelatin nanofiber mat, stabilized in fixed (left panels) and unfixed state (right panels) at 280°C, approached with different heating rates. All images were taken using a nominal magnification of 5000x.

	Fixed	Unfixed
0.5°C/min	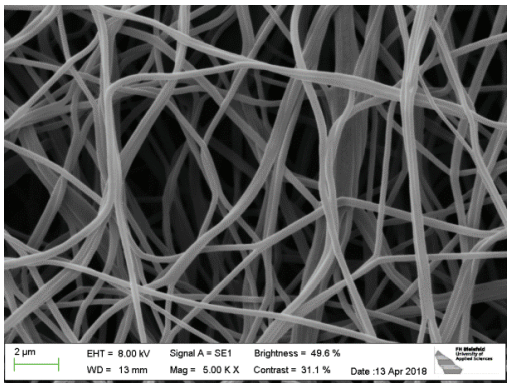	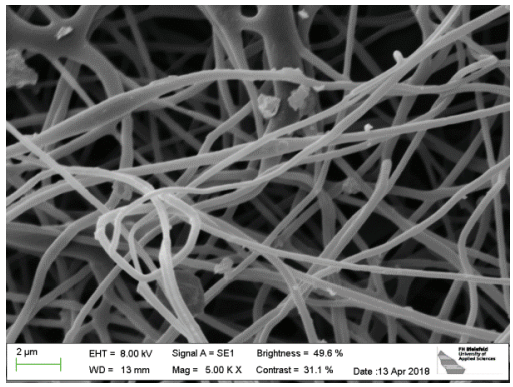
1°C/min	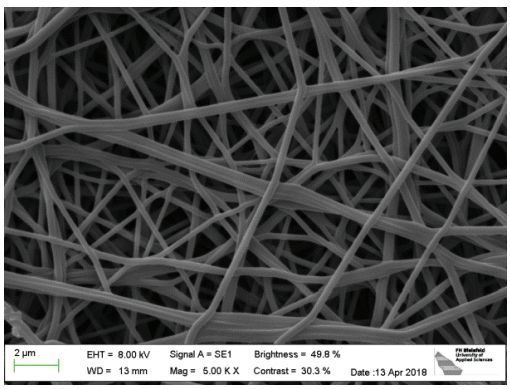	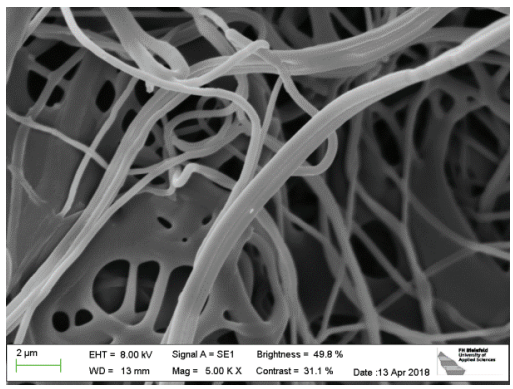
2°C/min	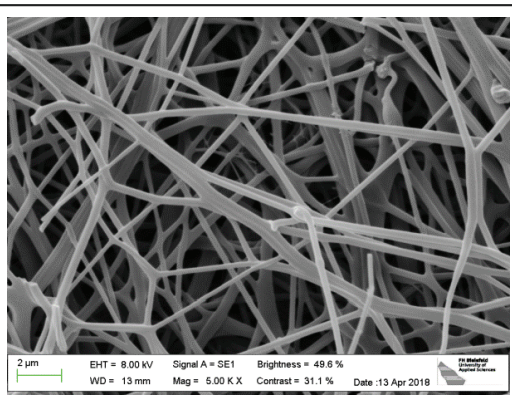	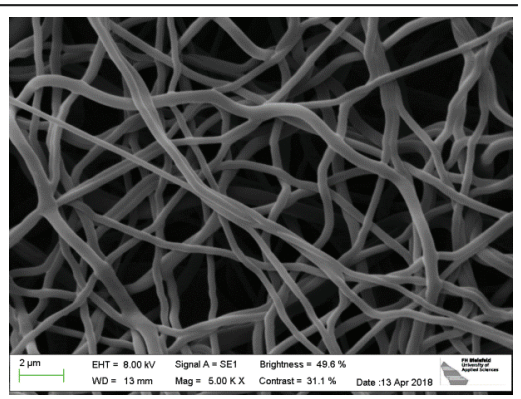
4°C/min	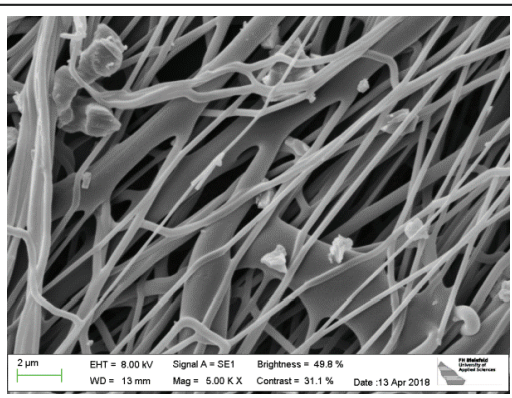	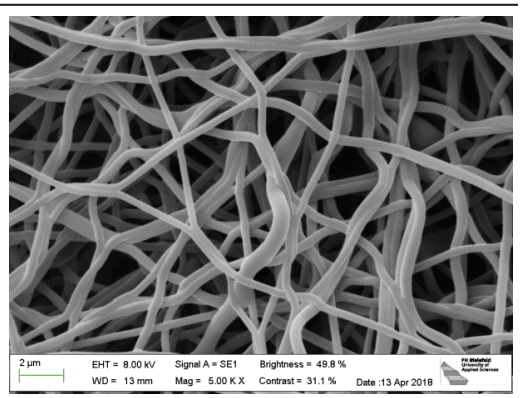

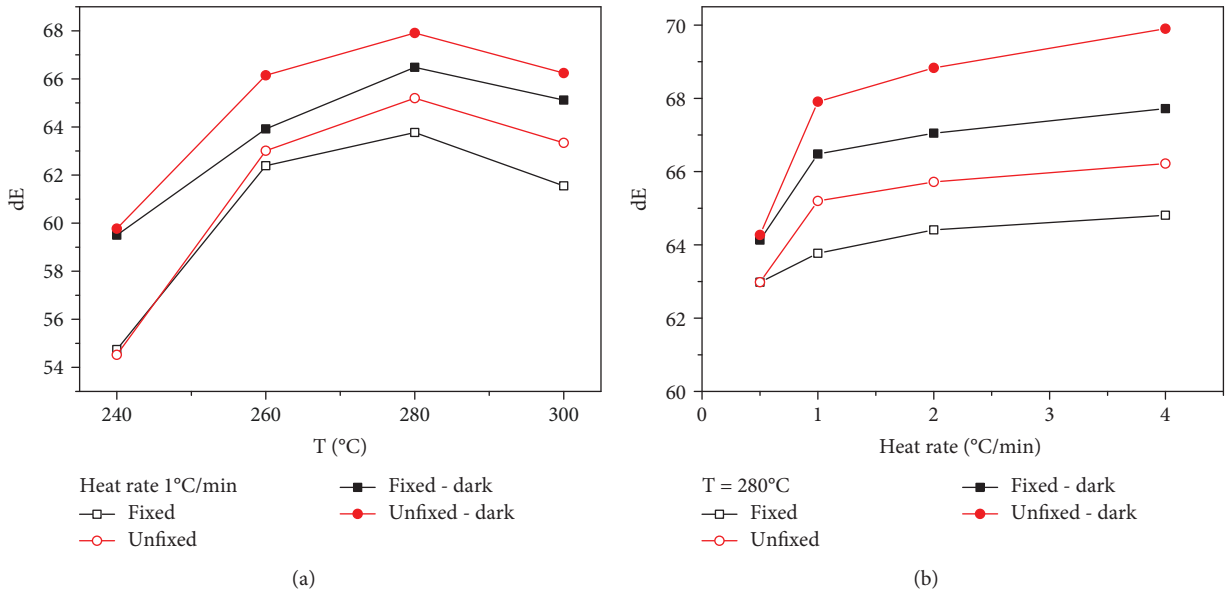

Figure 9: Color differences dE of samples stabilized at different end temperatures (a) and different heating rates (b) and isothermal treatment at the maximum temperature for 1 h.

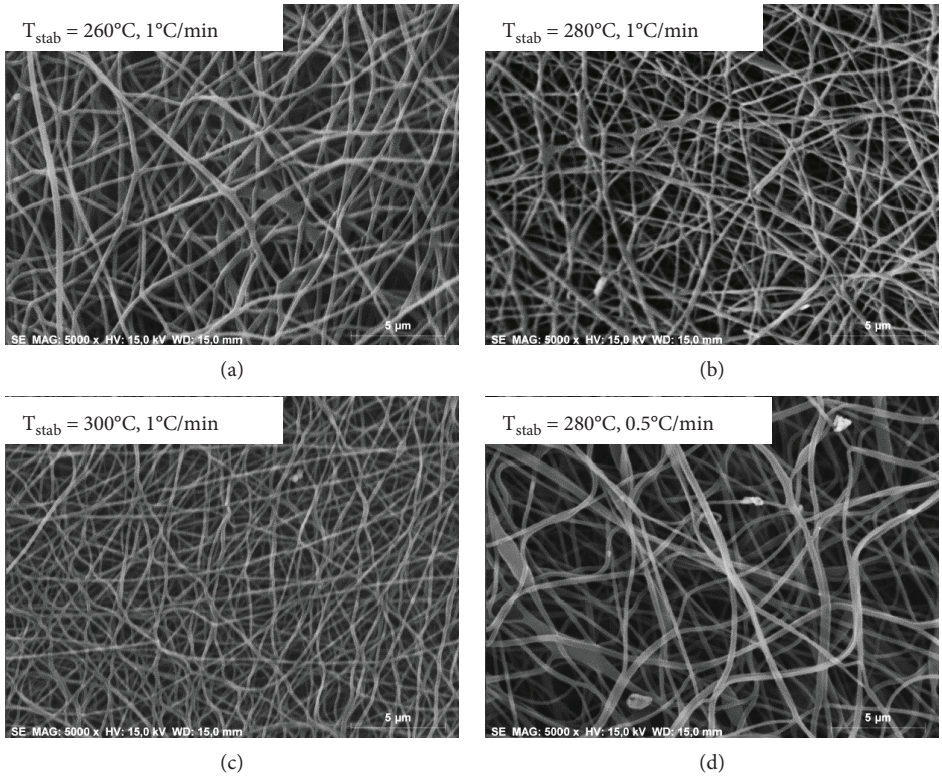

Figure 10: SEM images of some samples carbonized at 800°C.

increased heating rates, for which larger amounts of residual gelatin were found in the FTIR measurements (Figure 6).

It should be mentioned that for the smallest heating rate of 0.5°C/min as well as for the lowest temperature of 240°C (i.e., below the start of the gelatin degradation), there are no differences between fixed and unfixed samples visible. This may indicate that under these stabilization conditions, the fixation of the samples is not necessary to gain straight fibers without undesired meandering.

Finally, some of the optimally stabilized samples (all fixed during stabilization) were carbonized at a temperature of 800°C. Figure 10 depicts the SEM images taken after carbonization.

Table 5: Stabilization and carbonization yields as well as overall yield after the whole process for the samples depicted in Figure 10.

	Stabilization yield	Carbonization yield	Overall yield
T_{stab} = 260°C, 1°C/min	79.8%	14.3%	11.3%
T_{stab} = 280°C, 1°C/min	74.8%	36.4%	27.2%
T_{stab} = 300°C, 1°C/min	64.9%	25.0%	16.2%
T_{stab} = 280°C, 0.5°C/min	71.8%	28.6%	20.5%

Comparing these images, it is clearly visible that thicker fibers are achieved by smaller stabilization temperatures (260°C) and lower heating rates (0.5°C/min). This corresponds to the results of the stabilization process, as depicted in Tables 3 and 4, and suggests future tests combining relatively low stabilization temperatures and heating rates to support this property. This result clearly shows that by carefully choosing the stabilization conditions, the intended increase of the fiber diameter can survive the stabilization process, while the blending material responsible for this diameter increase melts at much lower temperatures.

On the other hand, these properties must be balanced against the carbonization yields. Here, we found the values given in Table 5.

According to these numbers, a stabilization temperature of 280°C in combination with a stabilization heating rate of 1°C/min should be preferred. The temperature of 260°C results in a small carbonization yield, while the highest temperature of 300°C leads to a reduced stabilization yield. Comparing both alternatives resulting in relatively thick fibers, a small heating rate of 0.5°C/min in combination with the typical stabilization temperature of 280°C is preferable since the overall yield is nearly twice as high as in the case of the lower stabilization temperature.

Figure 11 shows the results of FTIR measurements on the samples depicted in Figure 10. After stabilization, the peaks visible after stabilization are nearly vanished. Only very few functional groups are left after this process, corresponding to the high absorbance of carbon, as it is well known from the carbonization process of PAN and other carbon precursors [28, 29]. It should be mentioned that the small peaks visible here are neither identical with those stemming from PAN nor stabilized PAN nor gelatin, showing that the samples are carbonized to a high degree.

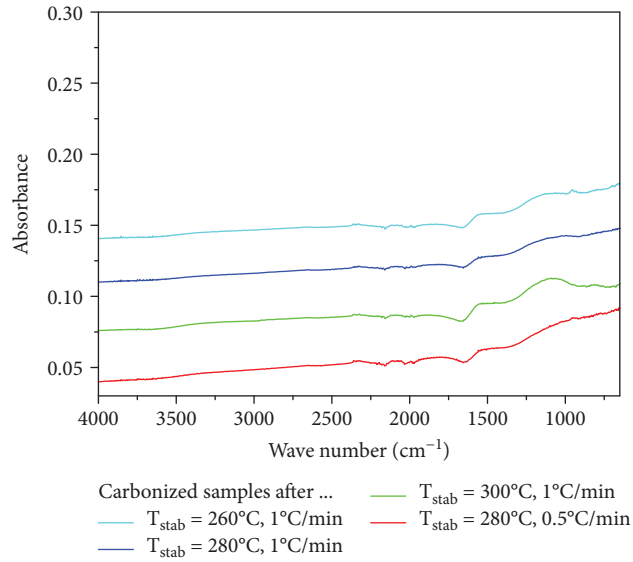

Figure 11: FTIR results of the samples carbonized at 800°C. The lines are offset vertically for clarity.

4. Conclusion

In this study, we have investigated electrospun PAN/gelatin nanofiber mats in terms of stabilization parameters and their influences on the resulting stabilized nanofibers. In all cases, the amount of gelatin was significantly reduced, especially above the onset of gelatin degradation at 250°C, as revealed by FTIR, CLSM, and SEM measurements. While adding gelatin did not result in creating porous PAN nanofibers after stabilization, we showed that using PAN/gelatin blends as precursors for carbon nanofibers offer a new possibility to create long, straight fibers without many undesired conglutinations. Future tests will concentrate on investigating the influence of the PAN : gelatin ratio on stabilization and subsequent carbonization processes.

Data Availability

All data used for the investigation are completely shown in the manuscript.

Conflicts of Interest

The authors declare that there is no conflict of interest regarding the publication of this paper.

Acknowledgments

The work was partly supported by the HiF funding of Bielefeld University of Applied Sciences. The authors acknowledge gratefully the program FH Basis of the German Federal Country North Rhine-Westphalia for funding the "Nanospider Lab." We also acknowledge the Junta de Andalucía for the financial support to the group TEP-184.

References

[1] J. He, W. Wang, R. Shi et al., "High speed water purification and efficient phosphate rejection by active nanofibrous membrane for microbial contamination and regrowth control," *Chemical Engineering Journal*, vol. 337, pp. 428–435, 2018.

[2] E. M. Cagil, F. Ozcan, and S. Ertul, "Fabrication of calixarene based protein scaffold by electrospin coating for tissue engineering," *Journal of Nanoscience and Nanotechnology*, vol. 18, no. 8, pp. 5292–5298, 2018.

[3] G. Potjewyd, S. Moxon, T. Wang, M. Domingos, and N. M. Hooper, "Tissue engineering 3D neurovascular units: a biomaterials and bioprinting perspective," *Trends in Biotechnology*, vol. 36, no. 4, pp. 457–472, 2018.

[4] H. Tang, W. Chen, J. Wang, T. Dugger, L. Cruz, and D. Kisailus, "Electrocatalytic N-doped graphitic nanofiber – metal/metal oxide nanoparticle composites," *Small*, vol. 14, no. 11, article 1703459, 2018.

[5] Y. Li and Y. Zheng, "Preparation and electrochemical properties of polyaniline/reduced graphene oxide composites," *Journal of Applied Polymer Science*, vol. 135, no. 16, article 46103, 2018.

[6] Y. Li, J. Ji, Y. Wang, R. Li, and W. H. Zhong, "Soy protein-treated nanofillers creating adaptive interfaces in nanocomposites with effectively improved conductivity," *Journal of Materials Science*, vol. 53, pp. 8653–8665, 2018.

[7] H. Wang, Y. Jiang, and A. Manthiram, "Long cycle life, low self-discharge sodium–selenium batteries with high selenium loading and suppressed polyselenide shuttling," *Advanced Energy Materials*, vol. 8, no. 7, article 1701953, 2018.

[8] S. Yao, J. Cui, J. Huang et al., "Rational assembly of hollow microporous carbon spheres as P hosts for long-life sodium-ion batteries," *Advanced Energy Materials*, vol. 8, no. 7, article 1702267, 2018.

[9] K. Wu, Y. Hu, Z. Shen et al., "Highly efficient and green fabrication of a modified C nanofiber interlayer for high-performance Li–S batteries," *Journal of Materials Chemistry A*, vol. 6, no. 6, pp. 2693–2699, 2018.

[10] X. Song, S. Wang, G. Chen et al., "Fe-N-doped carbon nanofiber and graphene modified separator for lithium-sulfur batteries," *Chemical Engineering Journal*, vol. 333, pp. 564–571, 2018.

[11] L. Zhu, L. You, P. Zhu, X. Shen, L. Yang, and K. Xiao, "High performance lithium–sulfur batteries with a sustainable and environmentally friendly carbon aerogel modified separator," *ACS Sustainable Chemistry & Engineering*, vol. 6, no. 1, pp. 248–257, 2018.

[12] Y. Zhao, Y. Liu, C. Tong et al., "Flexible lignin-derived electrospun carbon nanofiber mats as a highly efficient and binder-free counter electrode for dye-sensitized solar cells," *Journal of Materials Science*, vol. 53, no. 10, pp. 7637–7647, 2018.

[13] F. J. García-Mateos, R. Berenguer, M. J. Valero-Romero, J. Rodríguez-Mirasol, and T. Cordero, "Phosphorus functionalization for the rapid preparation of highly nanoporous submicron-diameter carbon fibers by electrospinning of lignin solutions," *Journal of Materials Chemistry A*, vol. 6, no. 3, pp. 1219–1233, 2018.

[14] W. Fang, S. Yang, T. Q. Yuan, A. Charlton, and R. C. Sun, "Effects of various surfactants on alkali lignin electrospinning ability and spun fibers," *Industrial & Engineering Chemistry Research*, vol. 56, no. 34, pp. 9551–9559, 2017.

[15] T. Grothe, D. Wehlage, T. Böhm, A. Remche, and A. Ehrmann, "Needleless electrospinning of PAN nanofibre mats," *Tekstilec*, vol. 60, no. 4, pp. 290–295, 2017.

[16] L. Sabantina, J. R. Mirasol, T. Cordero, K. Finsterbusch, and A. Ehrmann, "Investigation of needleless electrospun PAN nanofiber mats," in *AIP Conference Proceedings*, vol. 1952, article 020085, Secunderabad, India, 2018.

[17] C. Liu and K. Lafdi, "Fabrication and characterization of carbon nanofibers from polyacrylonitrile/pitch blends," *Journal of Applied Polymer Science*, vol. 134, no. 42, article 45388, 2017.

[18] Y. W. Ju and G. Y. Oh, "Behavior of toluene adsorption on activated carbon nanofibers prepared by electrospinning of a polyacrylonitrile-cellulose acetate blending solution," *Korean Journal of Chemical Engineering*, vol. 34, no. 10, pp. 2731–2737, 2017.

[19] D. Wehlage, R. Böttjer, T. Grothe, and A. Ehrmann, "Electrospinning water-soluble/insoluble polymer blends," *AIMS Materials Science*, vol. 5, no. 2, pp. 190–200, 2018.

[20] L. Yu and L. Gu, "Effects of microstructure, crosslinking density, temperature and exterior load on dynamic pH-response of hydrolyzed polyacrylonitrile-*blend*-gelatin hydrogel fibers," *European Polymer Journal*, vol. 45, no. 6, pp. 1706–1715, 2009.

[21] A. Bigi, G. Cojazzi, S. Panzavolta, K. Rubini, and N. Roveri, "Mechanical and thermal properties of gelatin films at different degrees of glutaraldehyde crosslinking," *Biomaterials*, vol. 22, no. 8, pp. 763–768, 2001.

[22] E. Cipriani, M. Zanetti, P. Bracco, V. Brunella, M. P. Luda, and L. Costa, "Crosslinking and carbonization processes in PAN films and nanofibers," *Polymer Degradation and Stability*, vol. 123, pp. 178–188, 2016.

[23] K. Mólnar, B. Szolnoki, A. Toldy, and L. M. Vas, "Thermochemical stabilization and analysis of continuously electrospun nanofibers," *Journal of Thermal Analysis and Calorimetry*, vol. 117, no. 3, pp. 1123–1135, 2014.

[24] G. S. Al-Saidi, A. Al-Alawi, M. S. Rahman, and N. Guizani, "Fourier transform infrared (FTIR) spectroscopic study of extracted gelatin from shaari (*Lithrinus microdon*) skin: effects of extraction conditions," *International Food Research Journal*, vol. 19, pp. 1167–1173, 2012.

[25] L. Sabantina, M. Rodríguez-Cano, M. Klöcker et al., "Fixing PAN nanofiber mats during stabilization for carbonization and creating novel metal/carbon composites," *Polymers*, vol. 10, no. 7, p. 735, 2018.

[26] C. Peña, K. de la Caba, A. Eceiza, R. Ruseckaite, and I. Mondragon, "Enhancing water repellence and mechanical properties of gelatin films by tannin addition," *Bioresource Technology*, vol. 101, no. 17, pp. 6836–6842, 2010.

[27] S. Gautam, A. K. Dinda, and N. C. Mishra, "Fabrication and characterization of PCL/gelatin composite nanofibrous scaffold for tissue engineering applications by electrospinning method," *Materials Science and Engineering: C*, vol. 33, no. 3, pp. 1228–1235, 2013.

[28] S. N. Arshad, M. Naraghi, and I. Chasiotis, "Strong carbon nanofibers from electrospun polyacrylonitrile," *Carbon*, vol. 49, no. 5, pp. 1710–1719, 2011.

[29] C.-W. Park, W.-J. Youe, S.-Y. Han, Y. S. Kim, and S.-H. Lee, "Characteristics of carbon nanofibers produced from lignin/polyacrylonitrile (PAN)/kraft lignin-g-PAN copolymer blends electrospun nanofibers," *Holzforschung*, vol. 71, no. 9, pp. 743–750, 2017.